
13th World Conference on Earthquake Engineering
Vancouver, B.C., Canada
August 1-6, 2004
Paper No. 995

# STRUCTURAL CONTROL USING REGENERATIVE FORCE ACTUATION NETWORKS

**J.T. SCRUGGS[1] and W.D. IWAN[2]**

## SUMMARY

Much of the research in semiactive control has made use of mechanical devices with parameters that may be varied so as to dissipate energy in a controlled manner. However, it is also possible for energy to be electrically dissipated by using electric motors to facilitate electromechanical energy conversion and electrical circuitry to control dissipation. This approach has an advantage in the sense that if two or more actuators are used to control a structure, their associated electrical circuitry may be connected such that they can share power. This allows one actuator to remove energy from the structure while another injects some of that energy back into the structure at another location.

Such systems are referred to as *Regenerative Force Actuation* (RFA) networks. The RFA networks considered in this paper employ rotational brushless DC machines with linear-to-rotational conversions. The dissipation and power flow in the electrical network is controlled through highly-efficient transistor switches. Although RFA networks are capable of facilitating large power flows, they typically require very little external power for operation.

There are several distinct ways in which RFA networks may be distributed throughout a structure to control vibrations. Actuators may be placed between stories, they may be used to excite secondary structures or mass dampers, and they may be used to interface with energy storage components (such as flywheels). In this paper, some simulation examples are presented which illustrate the capability of RFA networks to effectively control a three-story structure subjected to earthquake loading. The ability of the actuators in the network to share power is shown to provide a distinct advantage in transient simulations.

## 1. INTRODUCTION

In the last decade, a new class of forcing devices, first formally defined by Jolly and Margolis [1], has been proposed for use in structural control. Called *Regenerative Force Actuation* (*RFA*), such devices are capable of two-way power flow, like active devices. However, regenerative actuators possess energetic constraints which limit their forcing capability in a way which makes them distinct from active systems. Like semiactive systems, RFA networks have external power supply demands which are orders of magnitude less than their power flow capabilities, making them a compromise between active and

[1] Res. Asst., Div. of Eng. & Appl. Sci., California Instutute of Technology
[2] Prof. of Appl. Mech., Div. of Eng. & Appl. Sci., California Instutute of Technology

passive systems. Many of the favorable power and reliability traits of semiactive actuators extend to regenerative ones. However, they have two characteristics which set them apart from semiactive devices:

1) *Energy storage and reuse:* Semiactive devices must always remove structural energy. However, RFA networks have the capability of storing at least a fraction of the mechanical energy they remove from the structure, and of re-injecting that energy back into the structure at a later time. This is illustrated as configuration 1 in Figure 1, which depicts a 2-actuator RFA network which electrically interfaces an interstory actuator and an energy storage flywheel.
2) *Power coupling in networks:* When multiple regenerative actuators are distributed throughout a structure, they are capable of "sharing" power with each other. This enables one device to remove energy from a structure while another device at another location simultaneously re-injects that energy back into the structure. This is illustrated as configuration 2 in Figure 1, which depicts a 2-actuator RFA network which electrically interfaces an interstory actuator with a hybrid mass damper on the roof of the structure.

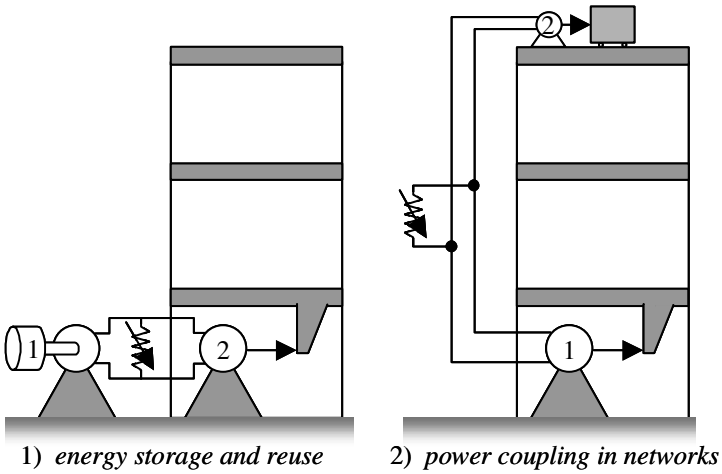


**Figure 1: Example configurations for RFA networks**

Regenerative actuation is still rather new in structural control applications [2]. It has been examined in the context of automotive suspension systems using a hydraulic regenerative actuator [3] and an electromechanical regenerative actuator [4]. Studies have also been conducted in the context of small, flexible structures with the use of a piezoelectric actuator with an inductor for energy storage [5]. In the various studies concerning this subject, there exist some differences as to what qualifies an actuation system as "regenerative." These discrepancies arise from how the energy storage system is modeled (if it is included at all), whether multiple actuators are considered, and if so, whether they are allowed to share power.

In the area of vehicle suspensions regenerative actuators has been defined as a network of force actuators which has power-coupled capability (i.e. trait 2 above) and which possesses a single, global, ideal energy storage device [1,3]. By "ideal," the implication is that this storage device possesses no dynamics, has 100% efficiency, and has no upper limit on energy capacity. The emphasis has been on steady-state disturbance rejection problems, and the energetic constraints of the devices are handled by classifying linear feedback control laws for which, in stationary excitation, the energy stored in the power supply tends to increase.

In civil engineering applications, regenerative actuators have been investigated by Nerves and Krishnan [6] and Scruggs and Lindner [7]. These studies considered one force actuator with access to a local energy storage, as in the aforementioned suspension research, this energy storage device was considered to be ideal. However, the study in [7] examined the implications of the fact that the energy storage system has a limited size, resulting in saturation and exhaustion of the supply system. It is also

important to mention that in the civil engineering area, studies with regenerative actuators have been limited to a single device with local energy storage. The concept of power-sharing between actuators has yet to receive any significant attention.

The purpose of this paper is to present results of recent investigations in this area by the authors, to highlight the major findings, and to discuss the possibilities for continued research in this new area. First, the fundamental idea of RFA networks is explained in detail. Then, the characterization and modeling of a realistic RFA network is discussed. Several methods of structural control synthesis, which account for the forcing limitations of RFA networks, are presented. Following these preliminary discussions, an example is presented in which two simple structural control laws are employed for the control of a scale-model three-story structure with a two-actuator network. One of the actuators is placed between the ground and first floor, while the second is used to excite a hybrid mass damper at the top of the structure. This example demonstrates the power-sharing capability of RFA networks.

## 2. THE IDEAL RFA NETWORK

An ideal RFA network is shown in Figure 2. For each the actuator subsystems consists of a roller screw is used to interface an electric motor with a piston. As a result of this interface, the torque $T$ and rotational velocity $\omega$ of the motor are linearly related to the force $f$ and linear velocity $v$. The electrical terminals of the machine are connected to a circuit which contains controllable power-electronic switches. This circuit interfaces the stator coils of the machine with the voltage $V_S$. By alternating the positions of these switches, the electrical currents in the machine can be controlled. Ideally, the switches in the electronic drive circuit would require no power to operate. As such, control of the electronic drive circuit would ideally require no power. In actuality, there is some power demand associated with switching control, but it is orders of magnitude lower than the power flowing through the system. With the terminals $S$-$S'$ of each actuator subsystem connected in parallel, these subsystems are capable of sharing power with each other, through proper control of the electrical circuitry. Thus, the electrical energy generated by one device may be converted back into mechanical energy by another.

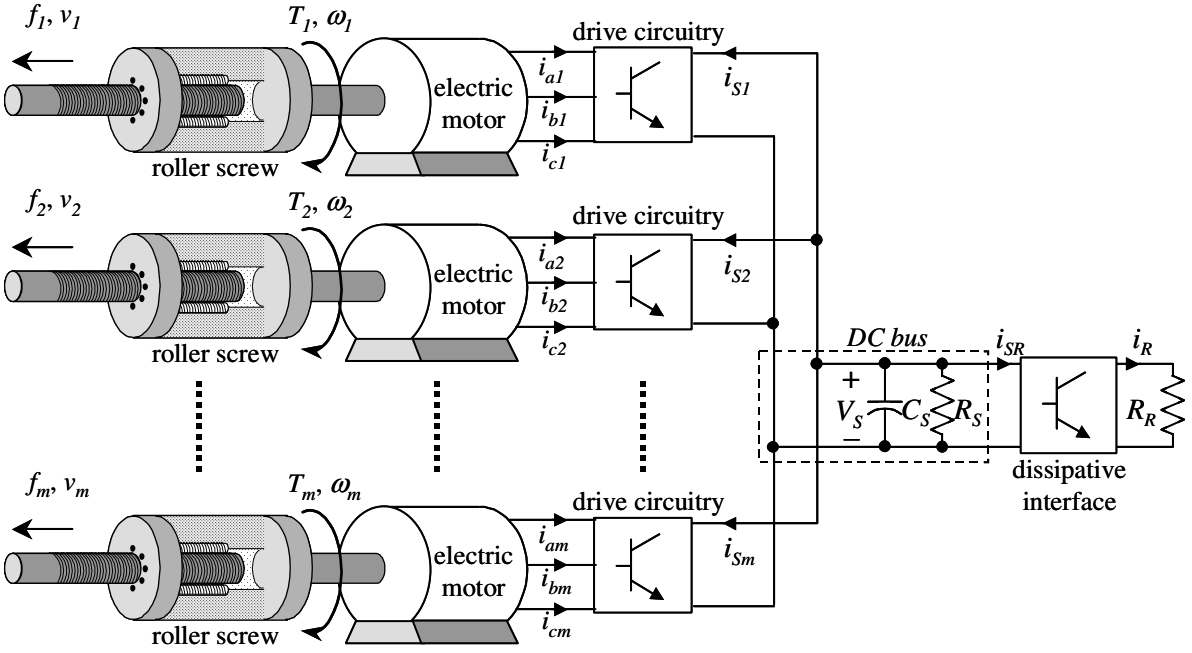


**Figure 2: Idealized electromechanical regenerative actuation system**

Each actuator subsystem undergoes a relative velocity $v_k$. The force vector is denoted by $\mathbf{f}_e = \{f_{e1}..f_{em}\}^T$ and the corresponding relative velocity vector is $\mathbf{v} = \{v_1...v_m\}^T$. For each actuator, the power injected into the structure is $P_k = f_{ek}v_k$. This mechanical power is converted from an electrical power $V_S i_{Sk}$. Ideally, this power conversion would be lossless and instantaneous, with $f_{ek}v_k$ being equal to $V_S i_{Sk}$. The terminals *S-S'* of all the machines are connected in parallel, and referred to as the *DC bus*, with voltage $V_S$. Also connected to the DC bus is a "dissipative interface" which is used to dissipate excess electrical energy generated by the actuators. This subsystem extracts current $i_{SR}$ from the DC bus, to produce a current $i_R$ through resistor $R_R$. Ideally, the dissipative interface would be lossless and instantaneous, with $V_S i_{SR}$ equal to $i_R^2 R_R$.

All the components of the electrical network (i.e. inside the boxes labeled "drive circuitry" and "dissipative interface" in Figure 2) are controlled by using transistors as electronic switches, as mentioned previously. Thus, ideally, control of these electronic networks consumes negligible power.

Remote energy storage and reuse is possible for this system. The simplest way to accomplish this is by designing one of the actuation subsystems as a flywheel drive system. Thus, the energy storage device becomes just another degree of freedom in the mechanical system to which the RFA network is connected. If an energy supply does not exist, or if it is saturated at its maximum storage level, excess electrical energy may be dissipated in a resistor bank, also connected to *S-S'*.

In Figure 2, capacitor $C_S$ is not intended to store any significant amount of energy, and resistor $R_S$ is selected to be sufficiently large, such that the energy it dissipates is minimal. Thus, the ideal RFA network is lossless and instantaneous, leading to the energy conservation constraint

$$\sum_{k=1}^{m} f_{ek} v_k = \mathbf{f}_e^T \mathbf{v} \leq 0 \tag{1}$$

For an ideal RFA network, the above relationship is the necessary and sufficient constraint for a force vector $\mathbf{f}_e$ to be feasible. The physical interpretation is that the total rate of energy injection into the structure (i.e. $\mathbf{f}_e^T\mathbf{v}$) must be negative. In other words, in the aggregate, the system must always generate electrical energy.

Of course, the power conversions in a real electromechanical system are not lossless. The electrical system also possesses significant dynamics and limitations which must be modeled. These issues constrain the system operation, producing realistic regenerative actuation constraints that are more restrictive and complex than the one in Eq. (1). However, the above discussion illustrates the general concept of regenerative actuation.

## 3. MODELING AND CHARACTERISTICS OF RFA NETWORKS

The ideal RFA network model discussed in the previous section assumed that the network could be operated at 100% efficiency. For instance, dissipation due to stator coil resistances and switching losses are ignored. Also, the dynamics of the electrical system are assumed to be instantaneous. In this section, a more accurate characterization will be discussed. The details of this characterization are contained in [8], and are only summarized here.

### Regenerative Forcing Constraint

The constraint of Eq. (1), which limits the feasible force vector $\mathbf{f}_e$, is called a *regenerative* constraint equation. If energy dissipation in the stator coils and switching circuitry are included in the RFA network model, this results in a more complicated regenerative constraint than Eq. (1), because in addition to the requirement that the system always generate electrical energy, there is the additional requirement that the system generate *enough* electrical energy to overcome the electrical dissipation incurred when power is transmitted from one device to another.

A more accurate model, which includes the electrical energy dissipation due to the resistances in the stator coils, results in the regenerative constraint equation

$$\mathbf{f}_e^T \mathbf{C}_c^{-1} \mathbf{f}_e + \mathbf{f}_e^T \mathbf{v} \le 0 \tag{2}$$

where

$$\mathbf{C}_c = \mathrm{diag}\left\{ \left( \frac{K_1}{l_1} \right)^2 \ \ldots \ \left( \frac{K_m}{l_m} \right)^2 \right\} \tag{3}$$

and where $K_i$ and $l_i$ are the motor constant and linear-to-rotational conversion lead, respectively, for actuator $i$. This quadratic equation has a useful graphical interpretation, as shown in Figure 3a for $m$=2. Also shown in the figure is the ideal regenerative constraint boundary, as the straight dotted line. The feasible force region is centered at a force vector equal to $-\frac{1}{2}\mathbf{C}_c\mathbf{v}$. The boundary of the ellipse intersects with the origin of $\mathbf{f}_e$-space in such a way as to be tangentially orthogonal to $\mathbf{v}$. Also note that the dimensions of the region grow linearly with the magnitude of $\mathbf{v}$.

Eq. (2) is a realistic equation for $\|\mathbf{v}\|$ large. However, for $\|\mathbf{v}\|$ small, the elliptical boundary is adversely distorted, which further constrains the capabilities of the system. This distortion is due to dissipation in the switches (i.e. the transistors and diodes). More accurate regenerative constraint equations may be derived which include these losses, but these expressions are much less mathematically tractable than Eq. (2), and control system synthesis methods, to be discussed in the next section, will in general use the simpler quadratic expression.

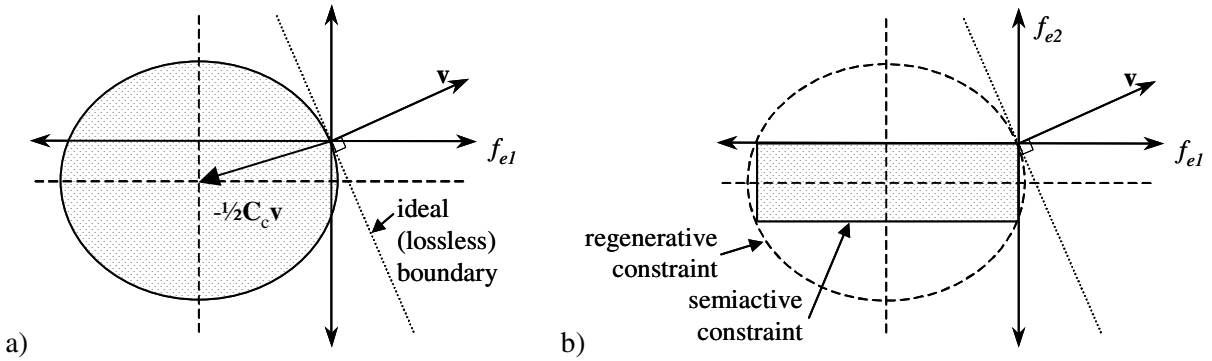


**Figure 3: Regenerative force constraint (a) and equivalent semiactive force constraint (b)**

**Comparison with Semiactive Forcing Constraint**

If the same devices used in the RFA network were not allowed to share power with each other (i.e. if they were all operated independently as dissipative devices) then each device's forcing constraints would be similar to those for mechanical semiactive devices. Operation in this manner, for a single device, was investigated by Scruggs and Iwan [9]. The benefit of the power-sharing capability of RFA networks can be easily ascertained by a comparison of the elliptical RFA constraint in Figure 3a with the corresponding feasible region for independent semiactive operation. This is shown in Figure 3b, which illustrates that the semiactive feasible force region is rectangular, intersecting with the regenerative constraint boundary on the force axes.

**Maximum Electromechanical Force**

In addition to the regenerative constraint imposed on the RFA network by energy conservation principles, there is also a constraint on the maximum force achievable for each device; i.e.

$$\left| \mathbf{f}_e \right| \le \mathbf{f}_{\max} \tag{4}$$

This maximum force constraint arises from a limitation on the amount of current which the stator coils of each machine can sustain without resulting in damage.

**Electrical System Dynamics**

In general, the electrical system will possess a much higher bandwidth than the mechanical system, and the dynamics of these two systems are resultantly uncoupled. Because the electrical dynamics are highly nonlinear, the marginal benefit obtained by including them in an analytical model for the actuation network is offset by a significant increase in the complexity of the system.

As an alternative, the approach in this research has been to treat the electrical and mechanical system dynamics separately, assuming them to be two decoupled systems. The switching control for the electrical system, and the system hardware itself, are designed such that the typical rise-time for the forces will be in the 1-10ms range. Then, for the design of the structural feedback control laws, the electrical system is assumed to have negligible dynamics. In transient simulations of the total system, however, a detailed dynamic model for the electronics can be used which explicitly simulates every switching operation, and which operates with a time step well below 1μs.

**Issues Pertaining to Switching Control**

The electrical quantities in the network are controlled through the toggling of transistor switches. The ultimate goal of the electronic control is to bring about high-bandwidth, zero-error tracking between $\mathbf{f}_e(t)$ and a desired force command $\mathbf{f}_e^*(t)$. Thus, the position of each electronic switch in the network is a nonlinear feedback function of the error $\mathbf{f}_e$-$\mathbf{f}_e^*$, as well as the velocity vector $\mathbf{v}$, the voltage $V_S$, and the current $i_R$.

Figure 4 shows a simple example simulation for the switching control system. This example corresponds to a 2-device RFA network, suitable for scale-model experiments. Both devices have power ratings of about 1kW. For this example, $\mathbf{v}$ is kept constant over the simulation duration and the system is commanded to realize a force command $\mathbf{f}_e^*$ as shown. The electrical quantities are all zero at the outset of the simulation. Both the trajectory in $\mathbf{f}_e$ space, as well as the transient plots, are shown. The most striking characteristic concerning the response is the high-frequency switching noise which is evident in all power-electronic systems. This noise, which is mostly concentrated at frequencies above 10kHz, is well outside the mechanical bandwidth of most structural applications.

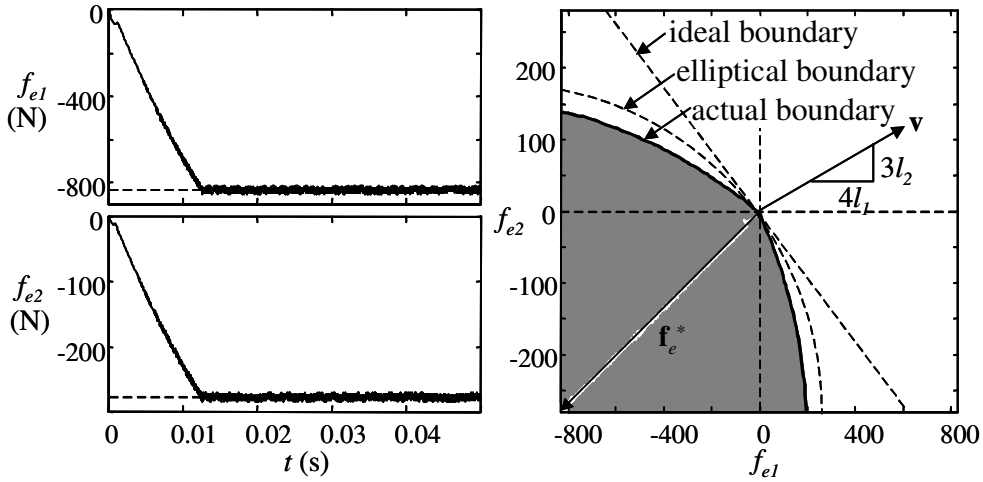


**Figure 4: Example of a transient electrical response for the electronic control system**

The design of control systems for these switches is a nontrivial task, because of uncertainties in the parameters of the system, and the time delay between sensory measurement and switch operation.

These uncertainty issues imply that the boundary of the feasible force region cannot be known precisely at any given time. But operation near the feasible force boundary is highly appealing because this operation corresponds to maximum-efficiency transmission of power from one actuator to another. It is therefore essential that an electronic control system be designed which, for $\mathbf{f}_e^*$ outside the feasible region, yields an error $\mathbf{f}_e$-$\mathbf{f}_e^*$ which is as small as possible. Also due to parameter uncertainty, limit cycles can arise for some control system design approaches, for $\mathbf{f}_e^*$ near the feasible region boundary. Of course, any realistic switching control system should be immune to these effects.

The resultant switching controller developed in this research is designed explicitly to circumvent these problems. The proposed control algorithm is centralized (as a consequence of the above issues) and may be classified as a variation on sliding-mode control.

Figure 5 shows a similar plot to that of Figure 4, except that now $\mathbf{f}_e^*$ is slightly outside the feasible region boundary. The two $\mathbf{f}_e(t)$ trajectories show the force histories for the case with (black) and without (gray) any robustness design. For the case without robustness, $\mathbf{f}_e(t)$ settles at approximately half its commanded value, even though $\mathbf{f}_e^*$ is only slightly outside the feasible region. With robustness, this error is considerably improved. The parameter $K$ is a control parameter which amplifies the effect of the robust controller. For large $K$, even better performance is possible.

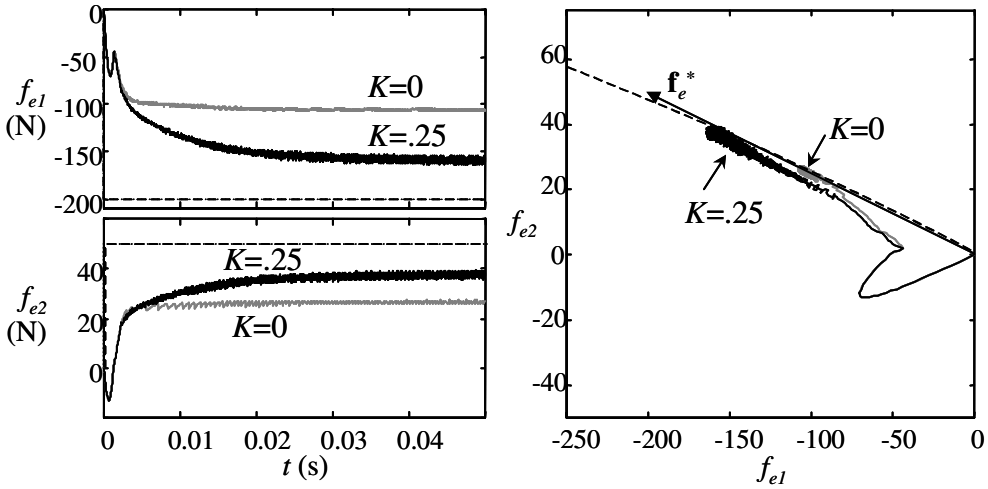


**Figure 5: Force tracking trajectories with (black) and without (gray) robustness to uncertainty**

The theory has been developed for arbitrary RFA networks (i.e. arbitrary scale and number of devices) although there are some remaining difficulties which remain unsolved for extremely large numbers of devices.

## 4. STRUCTURAL CONTROL ALGORITHMS

The capability of an RFA network to suppress deformations and high accelerations in a structure is directly dependent on the feedback control law, which relates the structural deformation measurements to the actuation force vector $\mathbf{f}_e$. In general, an assessment of the quality of an RFA network is inherently linked to the control law. Thus, in order to demonstrate the capabilities of an RFA network, it is necessary to first talk about the control system design methods employed in this research. In this section, two simple methods of control system design are briefly outlined, and the current direction of research in this area is discussed.

**Dynamic System Model**

Consider an arbitrary *n*-DOF base-excited shear structure equipped with an RFA network. The response of such the structure will be governed by

$$\mathbf{M}_{SA}\ddot{\mathbf{q}} + \mathbf{C}_{SA}\dot{\mathbf{q}} + \mathbf{K}_S\mathbf{q} = -\mathbf{M}_S\mathbf{G}a_g + \mathbf{N}\mathbf{f}_e \tag{5}$$

where $\mathbf{q}$ is the structural displacement vector relative to the base and $a_g$ is the base acceleration. The matrices $\mathbf{M}_{SA}$, $\mathbf{C}_{SA}$ and $\mathbf{K}_{SA}$ are the mechanical mass, damping, and stiffness matrices, and include the structural dynamics as well as the mechanical dynamics (i.e. inertia and damping) of the actuators. The matrix $\mathbf{N}$ also relates the actuation velocities $\mathbf{v}$ to the structural velocities, $\dot{\mathbf{q}}$, through

$$\mathbf{v} = \mathbf{N}^T\dot{\mathbf{q}} \tag{6}$$

**Effective Linear Damping Approach**

The simplest use of an RFA network is to impose supplemental linear damping to a structure. Consider a feedback control regime in which $\mathbf{f}_e$ is related to $\mathbf{v}$ through a square feedback matrix $\mathbf{Z}$, as

$$\mathbf{f}_e = -\mathbf{C}_c^{1/2}\mathbf{Z}\mathbf{C}_c^{1/2}\mathbf{v} \tag{7}$$

For $\mathbf{Z}$ constant, regenerative constraint (2) yields a constraint on $\mathbf{Z}$ which is necessary and sufficient to ensure that the above expression is feasible for all $\mathbf{v}$; i.e.

$$\overline{\sigma}\left(\mathbf{Z} - \tfrac{1}{2}\mathbf{I}\right) \le \tfrac{1}{2} \tag{8}$$

Satisfaction of Eq. (8) implies that $\mathbf{f}_e$, as related to $\mathbf{v}$ in Eq. (7), satisfies constraint (2).

If it can be assumed that $\mathbf{v}$ is sufficiently small, or $\mathbf{Z}$ is somehow additionally constrained such that $\mathbf{f}_e$ does not violate Eq. (4), then this "velocity feedback" approach fully characterizes the RFA network capability. This approach can be useful for a number of reasons. For some applications, such a formulation leads to a static feedback law (i.e. $\mathbf{Z}$ constant and pre-designed) which yields high performance in closed-loop. Such an implementation has certain advantages, in that it does not place large demands on control intelligence, and affords an implementation which potentially requires no structural sensors. Also, if $\mathbf{Z}$ is constant then the closed-loop system is linear time-invariant, which expedites an analysis of the structural response.

It is interesting to note that constraint (8) does not require $\mathbf{Z}$ to be diagonal or symmetric. Rather, an arbitrary asymmetric $\mathbf{Z}$ satisfying (8) will result in a feasible force $\mathbf{f}_e$. Thus, the damping matrices achievable with RFA networks are more general than those obtained with mechanical viscous dampers. For example, RFA networks can produce the illusion of viscous dampers connecting distant degrees of freedom. Additionally, the possible asymmetry of $\mathbf{Z}$, which results in an asymmetric structural damping, can be used to create dynamics which are mathematically similar to gyroscopic systems. Such dynamics do not have a clear analogy in traditional structural dynamics.

Clearly, different choices of $\mathbf{Z}$ will result in different levels of performance for the controlled system. In some circumstances, depending on the analytical definition of "performance" which is used, $\mathbf{Z}$ can be optimized through an asymptotic numerical algorithm. This involves similar concepts to those proposed by Skelton et.al. [10], except that $\mathbf{Z}$ is subjected to constraint (8). In Example 1 of this paper, this optimization is done for two different definitions of performance; mean-square structural drifts and mean-square accelerations.

**Clipped-Optimal Approach**

The effective linear damping approach is appealing because it yields a linear closed-loop system which has very clear and consistent analytical performance characteristics. However, the approach suffers from a disadvantage in that it considers only a very narrow class of feedback controllers. For instance, it

does not allow for explicit feedback of structural displacements, or of the full structural velocity vector. It is reasonable to expect that control laws which explicitly incorporate these structural states will result in further improvements in performance.

The Clipped-Optimal approach is the simplest approach which attempts to address these issues. It has been studied extensively in the context of semiactive systems in Civil Engineering [11], as well as in suspensions [12]. The method is illustrated in Figure 6, which shows that the feedback control law can be divided into two stages.

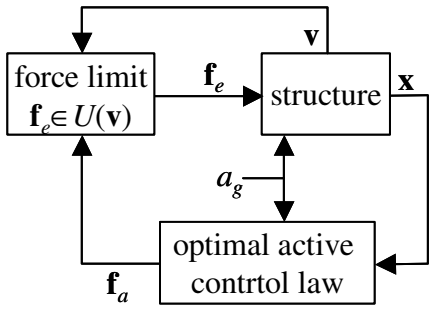


**Figure 6: Clipped-optimal feedback control**

In the first stage, the structural state vector **w** is measured and, from it, the intermediate force signal $\mathbf{f}_a$ is produced. The relationship between $\mathbf{f}_a$ and **w** is governed by the optimal active control law. For instance, for the quadratic performance measure

$$J = \int_0^\infty \left\{ \sum_{k=1}^{n} \left( \frac{d_k}{d_{k0}} \right)^2 + \sum_{k=1}^{n} \left( \frac{a_k}{a_{k0}} \right)^2 + \sum_{k=1}^{m} \left( \frac{f_k}{f_{k0}} \right)^2 \right\} dt \tag{9}$$

(where $d_k$ and $a_k$ are the interstory drift and absolute acceleration of floor $k$, and $f_k$ is the force for actuator $k$), the well-known full-information optimal LQG controller is a linear feedback function; i.e.

$$\mathbf{f}_a = \mathbf{K}\mathbf{w} \tag{10}$$

The second stage of clipped-optimal control is called the *clipping action*. The force signal $\mathbf{f}_a$ may not always be a feasible force (i.e. it may not satisfy Eqs. (2) and (4)). Thus, it must somehow be confined, or "clipped," to the feasible force region. There are many ways in which this clipping action may be accomplished, but the general idea is to make $\mathbf{f}_e$ as close to $\mathbf{f}_a$ as possible. Depending on the metric used to define "closeness," the clipping action operation will vary. Here, the clipping action is

$$\mathbf{f}_e = \underset{\tilde{\mathbf{f}}_e \text{ feasible}}{\arg\min} \left\| \tilde{\mathbf{f}}_e - \mathbf{f}_a \right\|_{\mathbf{R}} \tag{11}$$

where the norm $\|.\|_{\mathbf{R}}$ denotes the Euclidean norm with weighting matrix **R**.

Clipped-optimal control in general yields qualitatively favorable performance for integral-quadratic performance measures (i.e. mean-square quantities with nonzero force weighting), but theoretical upper bounds on this performance, and its departure from the optimal active performance, typically cannot be found. This is a major analytical drawback to this approach.

The performance of clipped-optimal controllers very much depends on the normalization constants $a_{k0}$, $d_{k0}$, and $f_{k0}$ in Eq. (9). As a general rule of thumb, a choice of weights which would yield extremely high-authority active control (i.e. matrices with $f_{k0}$ very small) do very poorly for the clipped-optimal system. And, of course, a choice of matrices resulting in extremely low authority active control also result in poor clipped-optimal performance. Thus, as with semiactive systems, the design of clipped-optimal control requires a fair amount of trial-and-error.

One way to intelligently go about formulating the expression for $J$ is to directly penalize controllers which operate far outside the elliptical boundary of the regenerative constraint, or which have high forces. This may be readily accomplished by augmenting $J$ to the expression

$$J = \int_0^\infty \left\{ \sum_{k=1}^{n} \left( \frac{d_k}{d_{k0}} \right)^2 + \sum_{k=1}^{n} \left( \frac{a_k}{a_{k0}} \right)^2 + \sum_{k=1}^{m} \left( \frac{f_k}{f_{k0}} \right)^2 + q_R \left( \mathbf{f}_e^T \mathbf{C}_c^{-1} \mathbf{f}_e + \mathbf{f}_e^T \mathbf{v} \right) \right\} dt \tag{12}$$

The last quadratic term (with nonnegative weighting factor $q_R$) is minimal when $\mathbf{f}_e = -\frac{1}{2}\mathbf{C}_c\mathbf{v}$ (i.e. when $\mathbf{f}_e$ is in the center of the feasible region) and increases quadratically as $\mathbf{f}_e$ deviates from this point. Thus, for $q_R$ infinitely large, the optimal control is $\mathbf{f}_e = -\frac{1}{2}\mathbf{C}_c\mathbf{v}$, which always meets the regenerative constraint. For $q_R$ finite, the effect of this term is to reduce $J$ for control systems which, on average, meet the regenerative constraint, and to increase $J$ for control systems which do not.

Note that in this discussion, full-information, noiseless feedback has been assumed. However, similar observations can be made for clipped-LQG controllers with noisy and/or incomplete measurements.

## 5. EXAMPLE OF RFA NETWORK APPLICATION

Consider the system shown in Figure 7. The structural model is taken from [11]. Actuators are installed at the base of the structure and at the mass damper. The actuation network involves electric machines with parameters identical to those used in [9]. Parameters for these actuators are shown in Figure 7.

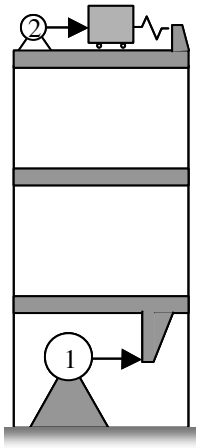


**Structural Characteristics:**

- Building is lightly damped (i.e. below 1% critical)
- Natural frequencies: 5.5, 15.8, & 23.6 Hz
- Model is scaled 1:5 in time, 2:7 in length
- TMD is 0.3% of building mass
- Natural frequency of TMD: 5.5 Hz

**Actuator Characteristics:**

| $i$ | 1 | 2 |
|---|---|---|
| $K_i$ (Nm/W$^{1/2}$) | 0.4858 | 0.4858 |
| $l_i$ (m/rad) | 0.0013 | 0.0067 |
| $\{\mathbf{C}_c\}_{ii}$ (Ns/m) | $1.32\times10^5$ | $5.31\times10^3$ |
| $f_{i\,max}$ (N) | 832.5 | 166.5 |

**Figure 7: Structural control example configuration**

For this system, two controllers were designed, using the effective damping (ED) and clipped-optimal (CO) control approaches. For both controllers, the same values of $a_{k0}$, $d_{k0}$, and $f_{k0}$ were used in the expression for $J$ in Eq. (9). For the ED controller, the $\mathbf{Z}$ matrix was optimized for minimum $J$, assuming the ground acceleration to be stationary noise with the Kanai-Tajimi spectrum. For the CO controller, the expression for $J$ was augmented, as in Eq. (12), to penalize active control matrices $\mathbf{K}$ which tend to result in violation of the regenerative constraint.

Additionally, the optimal passive damping case (PD) was found, in which both actuators are replaced with viscous dampers. As with the ED case, these dampers were optimized for minimum $J$, assuming the ground acceleration to be stationary noise with the Kanai-Tajimi spectrum.

For these three cases, the structural response was simulated for four earthquake records. Specifically, these are the El Centro (May 18, 1940, N-S component measured at Imperial Valley

Irrigation District), Hachinohe (May 16, 1968, N-S component measured at Hachinohe City), Kobe (Jan. 17, 1995, N-S component measured at Japanese Meteorological Agency station), and Northridge (Jan. 17, 1994, N-S component measured at Sylmar County Hospital) records. Because the structure represents a scale-model building, each record has been time-scaled by a factor of 5. Response results for the maximum drift and acceleration quantities for floors 1, 2, and 3, as well as the mass damper, are shown in Table 1. Also shown are the maximum forces for actuators 1 and 2 (or, in the PD case, the maximum force of the corresponding viscous damper). The results indicate that the CO and ED controllers result in better compromise between drift and acceleration than is achievable with the PD case. Although the PD case consistently yields lower first-story drifts (for all four earthquakes), it also consistently results in larger second- and third-story drifts. Additionally, the accelerations of the floors for the PD case are consistently higher than for the CO and ED cases.

Between the CO and ED cases, it is not clear which has the higher performance in general. The CO controller yields lower second- and third-story drifts and accelerations, but the ED controller gives better first-story quantities. Also, it is interesting that the ED controller consistently produces larger forces for both actuators. In general, the PD case produces larger forces than both controllers.

**Table 1: Earthquake response data for CO, ED, and PD cases**

| Earthquake | El Centro | | | Hachinohe | | | Kobe | | | Northridge | | |
|---|---|---|---|---|---|---|---|---|---|---|---|---|
| | CO | ED | PD | CO | ED | PD | CO | ED | PD | CO | ED | PD |
| $d_1$ (mm) | 1.01 | 0.94 | 0.99 | 0.94 | 0.89 | 0.88 | 5.51 | 5.33 | 3.63 | 2.92 | 2.60 | 2.81 |
| $d_2$ (mm) | 0.92 | 1.07 | 1.14 | 0.57 | 0.67 | 0.68 | 2.52 | 2.86 | 3.41 | 2.06 | 2.17 | 2.25 |
| $d_3$ (mm) | 0.62 | 0.72 | 0.80 | 0.45 | 0.48 | 0.49 | 1.46 | 1.73 | 1.99 | 1.39 | 1.50 | 1.62 |
| $d_d$ (mm) | 7.81 | 10.1 | 9.72 | 6.88 | 8.83 | 6.69 | 33.0 | 40.2 | 26.0 | 23.4 | 29.3 | 9.08 |
| $a_1$ (m/s$^2$) | 2.74 | 2.64 | 5.21 | 2.08 | 1.96 | 3.69 | 9.49 | 8.06 | 11.7 | 9.61 | 9.11 | 10.0 |
| $a_2$ (m/s$^2$) | 2.73 | 3.33 | 7.05 | 2.87 | 3.53 | 5.24 | 7.88 | 8.74 | 15.2 | 6.02 | 6.88 | 9.32 |
| $a_3$ (m/s$^2$) | 4.35 | 4.99 | 7.13 | 3.07 | 3.20 | 5.34 | 10.5 | 12.2 | 16.2 | 9.85 | 10.7 | 13.9 |
| $a_d$ (m/s$^2$) | 8.20 | 14.8 | 48.9 | 4.71 | 9.03 | 48.0 | 24.4 | 39.6 | 134 | 20.1 | 28.7 | 68.1 |
| $f_{e1}$ (N) | 517 | 575 | 739 | 385 | 430 | 454 | 888 | 953 | 194 | 870 | 916 | 1449 |
| $f_{e2}$ (N) | 56.5 | 95.3 | 2.23 | 29.0 | 42.9 | 1.34 | 141 | 179 | 5.68 | 106 | 166 | 5.54 |

Figure 8 shows the power flow for both actuators, as well as their combined power, for the ED case. (Recall that the convention here is that positive power conversion is from the electrical system to the mechanical system.) Results are similar for the CO case. Note that there are periods during which $P_2$ is significantly positive, indicating that during these times, energy is being delivered from the ground to the roof. However, as expected, the system obeys the ideal regenerative constraint, as evidenced by the fact that at $P_1+P_2$ is always negative.

To gain a better understanding of what is happening for time periods where $P_2>0$, consider Figure 9 which shows $P_2$, as well as the velocity $v_d$ of the mass damper (relative to the roof) for both the ED and the PD cases, for the El Centro earthquake record. Note that $v_d$ takes much longer to build up its amplitude for the PD case, as compared with the ED case, and that for early times when the magnitude of $v_d$ is increasing, $P_2>0$. This indicates that the RFA system is capable of exciting the mass damper into action more quickly. After two cycles of large oscillation of the mass damper, $P_2$ is more consistently negative, indicating that actuator 2 is removing energy from the structure for most of each oscillatory cycle. Thus, after quickly exciting the mass damper through power coupling, the RFA network reverts to a more traditional dissipative behavior.

Similar behavior is exhibited for the CO case, and for the other earthquake records. The general trend is in the responses is intuitive: During periods when the ground acceleration magnitude is growing, the RFA network delivers a significant amount of power from the ground to the roof. Likewise, during periods when the ground acceleration is small, the RFA network dissipates the structural energy.

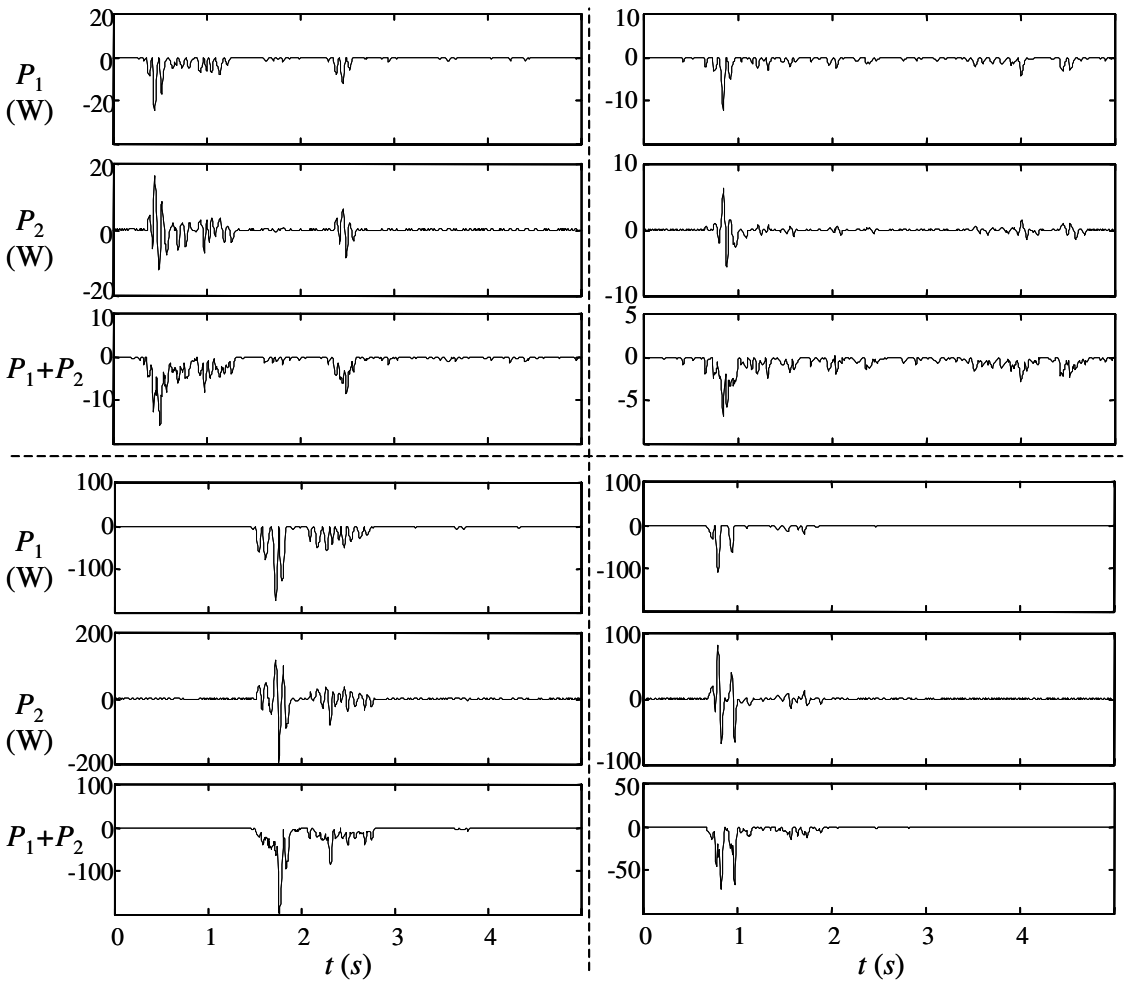


**Figure 8: Actuation power flows for the El Centro, Hachinohe, Northridge, and Kobe earthquakes (clockwise from top left)**

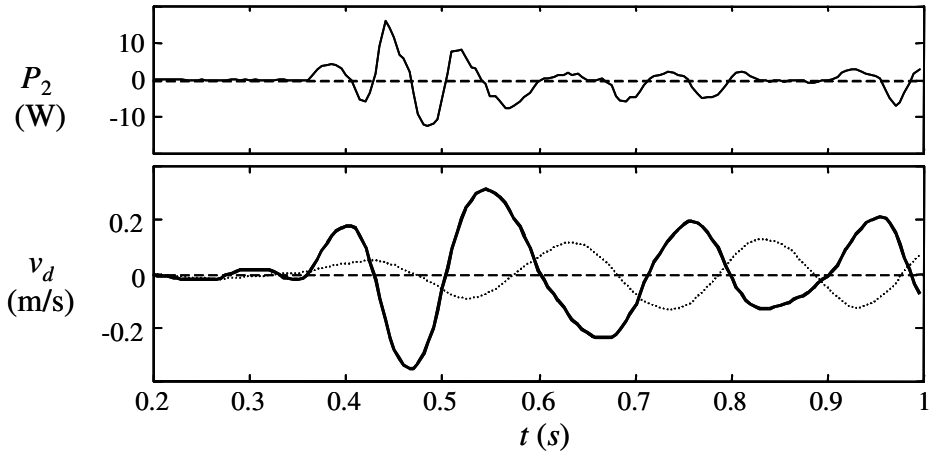


**Figure 9: Relative velocity of mass damper with ED solid (solid) and PD (dashed) cases, and the associated power flow, for the El Centro earthquake record**

## 6. CONCLUSIONS AND DISCUSSION

The main thrusts of this research have been: (1) the development of electronic control algorithms for high-precision force tracking, (2) the development of structural feedback control algorithms, and (3) an exploration of the relative effectiveness of RFA networks to improve energy-constrained control for various actuation configurations. The theoretical studies summarized in this paper suggest that there are unique traits of RFA networks which may make them highly appealing in certain high-performance structural control applications. The power-sharing capability of these systems opens up a new dimension in the areas of dissipative and energy-constrained control. There are a great many possible avenues for exploration concerning this topic.

All the components of the system are commonplace in many areas of industrial engineering, and are all commercially available. Thus, highly-accurate models of the various components of the system currently exist, making "proof of concept" experiments less crucial. However, the theory has reached the point where experimentation is the next logical step, and current research efforts are focused on the goal of developing novel actuators which are custom-designed for civil structure applications. Commercially available hardware is typically not optimally designed for such applications, which involve extremely high forces and low velocities.

The linear effective damping and clipped-optimal control approaches are appealing primarily because they are comparatively simple methods. In the case of effective linear damping, this simplicity is due to the linearity of the closed-loop differential equation. In the case of clipped-optimal control, it is due to the assumption that the clipping action does not significantly modify the favorability of an optimal linear-quadratic active control law. However, both methods are sub-optimal. In the case of linear effective damping, it is true that the **Z** matrix can be optimized for performance, but this effectively constitutes an optimization over a very small controller space. In the case of clipped-optimal control, it is in general very difficult to make analytical conclusions about the extent to which the clipped-optimal system performance adheres to the active optimal performance. Thus, there are a number of important issues concerning performance-optimal control system design for RFA networks and about the potential benefit of RFA networks for structural response improvement. The development of control system design methods which strike a better balance between mathematical tractability and performance is a current goal of research in this area.

## REFERENCES


1. Jolly, M.R. and D.L. Margolis, *Assessing the Potential for Energy Regeneration in Dynamic Subsystems.* Journal of Dynamic Systems, Measurement, and Control, 1997. 119(June): p. 265-270.
2. Wendel, G.R. and G.L. Stecklein, *A Regenerative Active Suspension System.* SAE Publication SP-861, 1991: p. 129-135.
3. Jolly, M.R. and D.L. Margolis, *Regenerative Systems for Vibration Control.* Journal of Vibration and Acoustics, 1997. 119(April): p. 208-215.
4. Okada, Y., H. Hideyuki, and S. Kohei, *Active and Regenerative Control of an Electrodynamic-Type Suspension.* JSME International Journal, C, 1997. 40(2): p. 272-278.
5. Wang, K.W., J.S. Lai, and W.K. Yu, An Energy-Based Parametric Control Approach to Structural Vibration Suppression via Semi-Active Piezoelectric Networks. Journal of Vibration and Acoustics, 1996. 118(July): p. 505-509.
6. Nerves, A.C. and R. Krishnan. A Strategy for Active Control of Tall Civil Structures Using Regenerative Electric Actuators. in Proc., Engineering Mechanics Conference. 1996. Fort Lauderdale, FL.

7. Scruggs, J. and D.K. Lindner. Active Energy Control for Civil Structures. in SPIE 1999 North American Symposium on Smart Structures and Materials: Smart Systems for Bridges, Structures, and Highways. 1999. Los Angeles, CA.
8. Scruggs, J.T. and W.D. Iwan, *Structural Control Using Regenerative Actuation Networks.* International Journal of Structural Control (submitted), 2003.
9. Scruggs, J.T. and W.D. Iwan, *Control of a Civil Structure Using an Electric Machine with Semiactive Capability.* ASCE Journal of Structural Engineering, 2003. 129(7): p. 951-959.
10. Skelton, R.E., B. Hanks, and M. Smith, *Structure Redesign for Improved Dynamic Response.* Journal of Guidance, Control and Dynamics, 1991. 15(5): p. 1272-1278.
11. Dyke, S.J., et al., Modeling and control of magnetorheological dampers for seismic response reduction. Smart Materials and Structures, 1996. 5: p. 565-575.
12. Tseng, H.E. and J.K. Hedrick, *Semi-active control laws - optimal and sub-optimal.* Vehicle System Dynamics, 1994. 23: p. 545-69.